Journal of Ceramic Science and Technology

Phase Evaluation of YSZ upon Doping with Ta^{5+}, Ti^{4+} and Ca^{2+} with Combined Raman and XRD Analysis

A. Bhattacharya[*1], T. Wermelinger[2], V. Shklover[1]

[1]Laboratory of Crystallography, Department of Materials, ETH Zürich, 8093 Zürich, Switzerland
[2]Institute of Nanometallurgy, Department of Materials, ETH Zurich, 8093 Zurich, Switzerland

Abstract

To improve the phase stability of 7YSZ (7 wt%-Y_2O_3-doped ZrO_2), it has been doped with larger (Ca^{2+}) and smaller (Ti^{4+} or Ta^{5+}) ions. Complementary Raman and XRD studies of these stabilized systems have been performed. The tetragonal symmetry of the Ta^{5+}-ion-doped YSZ sample and the Ti^{4+}-doped YSZ sample, and the cubic symmetry of Ca^{2+}-doped YSZ have been confirmed both by means of XRD and Raman analyses. Raman scattering measurements show shifts of characteristic peaks when the YSZ is doped with Ta^{5+}, Ti^{4+} and Ca^{2+} cations. The peak shift increased with increasing dopant concentration in the ZrO_2 lattice. The Ta-doped YSZ sample heat-treated below 1500 °C contained some $YTaO_4$ phase, which was confirmed by means of XRD as well as by Raman spectroscopy. The effect of Ca^{2+} ion doping on the Raman peak shift was much higher than that of Y^{3+} ion doping. In this work it has been highlighted that Raman spectroscopy is a useful tool complementing XRD, for qualitative comparison of the doping effect on the lattice parameters of ZrO_2.

Keywords: TBC, YSZ, Raman spectroscopy, XRD, ZrO_2

I. Introduction

ZrO_2 stabilized with cations of different valency has found application in many technologically important areas, e.g. as thermal barrier coatings (TBC). Pure zirconia exists as monoclinic phase at room temperature, however, when doped with cations such as Y^{3+}, metastable tetragonal (t′) and metastable cubic (c) phase can also exist at room temperature, depending on the amount of doping. 7YSZ is currently being used as TBC in gas turbine engines. 7YSZ consists of predominantly metastable 'non-transformable' t′ phase at room temperature, and undergoes transformation into transformable Y-deficient tetragonal t and Y-rich cubic c (fluorite) phases when treated for a relatively long time at and above ~ 1200 °C: t′ → t + c [1−3] The transformable t-phase of 7YSZ undergoes martensitic transformation to monoclinic phase (t → m) upon cooling accompanied with detrimental volume expansion (~ 4 − 5 %). In order to improve the lifetime of TBC further, many researchers have tried doping 7YSZ with cations such as TiO_2, Yb_2O_3, Ta_2O_5, and other oxides [1,4−6], which has improved the stability of these systems. Recent studies have shown that simultaneous doping of Y_2O_3 and Ta_2O_5 stabilizes the tetragonal ZrO_2 structure up to 1500 °C [6,7].

To understand the phase composition and stability of double-stabilized ZrO_2-based oxides, XRD is commonly used as a characterization technique. However, powder XRD is not sensitive enough to small oxygen anions displacements, which could lead to significant phase changes in ZrO_2. This is due to the low scattering factor of oxygen compared to that of Zr or other doping cations. On the other hand, Raman microscopy is highly sensitive to oxygen displacements, which lead to a change of polarization and intermediate range ordering without long range periodicity [8]. For example, t″ phase in ZrO_2 doped with 16 mol% $YO_{1.5}$ was detected with Raman spectroscopy but is not detectable with XRD [9]. The t″ phase is a pseudo cubic phase with a c/a ratio equal to 1 but has to be considered tetragonal because of oxygen anions displacements. Another advantage of Raman microscopy is the high lateral resolution of the method which allows chemical information to be obtained in the submicrometer range.

A lot of work has been done on Raman studies of ZrO_2-based systems. Also the effect of doping of tetragonal zirconia solid solutions on their Raman spectra has been studied [10]. It was shown that the addition of Y^{3+} cations does not change the peak positions in the Raman spectra. Y^{3+} cations are bigger than the Zr^{4+} cations and their addition increases the metal-oxygen bond lengths but the formation of oxygen vacancies forces zirconium cations to gain a smaller coordination number than the usual eight. These two effects counterbalance each other and no shifts of the peaks in the Raman spectra were observed. However, adding Ta^{5+} or Nb^{5+} cations leads to a change of the local environment of metal cations. A Ta^{5+} cation, which is smaller than a Zr^{4+} cation, tends to be tetrahedrally coordinated whereas Zr^{4+} or Y^{3+} cations retain their coordination number of eight. Hence, in the Raman spectra only the shifts of the characteristic peaks at 260 or 640 cm^{-1} are

* Corresponding author: anup.bhattacharya@mat.ethz.ch

seen. These peaks belong to stretching modes of vibration of Zr-O′ and Zr-O bonds, respectively [11].

This work reports on the Raman spectroscopic characterization of (Y^{3+}, Ta^{5+})- and (Y^{3+}, Ca^{2+})-doped ZrO_2 along with XRD phase analysis. The effect of the dopant concentration on the Raman spectra has also been demonstrated.

II. Experimental

TaYSZ with 16 mol% Ta and 16 mol% Y were prepared by means of reverse co-precipitation. $ZrOCl_2.8H_2O$ (99.9 %, Alfa-Aesar GmbH, Karlsruhe, Germany), $Y(NO_3)_3.6H_2O$ (99.9 %, Alfa-Aesar GmbH, Karlsruhe, Germany) and $TaCl_5$ (99.99 %, Sigma-Aldrich GmbH, Steinheim, Germany) were used as precursors for precipitation of corresponding hydroxides of Zr, Y and Ta, respectively. The precursors were mixed in an ethanol solution and slowly dropped into an ammonia solution at pH 10. The precipitates were washed thoroughly, dried overnight and calcined at 1000 °C for 4 h. Calcined powders were annealed at temperatures from 1100 °C to 1500 °C for 4 h. Long-term annealing of the powders was performed at 1250 °C for 600 h. For all the heat treatments, the heating and cooling rates were maintained at 10 K/min. Phases formed at different temperatures were analyzed with an X-ray powder diffractometer (Xpert Pro PANalytical, 7600 AA ALMELO, the Netherlands).

TiYSZ with 7 mol% TiO_2 and 7 mol% $YO_{1.5}$ was synthesized with a similar technique. Titanium iso propoxide (99.995 %, Alfa-Aesar GmbH, Karlsruhe, Germany) was used as a precursor for the TiO_2 component.

$YTaO_4$ was also prepared with the same method and the precursors used were equal amounts of $Y(NO_3)_3 \cdot 6H_2O$ and $TaCl_5$ (99 %, Alfa Aesar, Germany). CaYSZ was prepared by means of reverse coprecipitation with precursors: calcium chloride ($CaCl_2 \cdot H_2O$, 99+ % for analysis, ACROS Organics), yttrium nitrate [$Y(NO_3)_3 \cdot H_2O$, 99.9 % REO, Alfa Aesar] and zirconium oxychloride ($ZrOCl_2 \cdot H_2O$, 99.9 % metal basis, Alfa Aesar). NaOH was used as the precipitating agent in CaYSZ synthesis.

CaYSZ was also synthesized by means of solid state synthesis. Appropriate amounts of calcium carbonate ($CaCO_3$, Puratronic® 99.997 % metal basis, Alfa Aesar), yttrium oxide (Y_2O_3, REactan® REO 99.999 %, Alfa Aesar) and zirconium oxide (ZrO_2, Puratronic© 99.978 %, Alfa Aesar) were ball-milled for 24 h with ethanol as the mixing agent. The milled powder was filtered, dried and calcined for 6 h at 1000 °C. The calcined powder was then sintered for 36 h at 1600 °C to obtain the single phase. Commercial 7YSZ and CaSZ (com) were used (HC Stark GmbH, Germany).

Raman analyses were performed using a Raman microscope CRM 200 (WITec, Germany) equipped with a continuous He-Cd laser with a wavelength of 442 nm.

III. Results and Discussion

The Raman spectra of TaYSZ (1500 °C, 4 h), TiYSZ (1200 °C, 4 h) and 7YSZ (commercial) are shown in Fig. 1. These spectra indicate their tetragonal symmetry [10]. 7YSZ features five characteristic peaks at 263, 320, 464, 606 and 640 cm⁻¹ as reported earlier [12]. It can be seen that peaks

at 260 cm⁻¹ and 640 cm⁻¹ are shifted to higher wave numbers when YSZ is doped with TiO_2. These peaks correspond to non-equivalent Zr-O′ and Zr-O bonds. Their shift to higher energy indicates stronger Zr-O bonding. This could be explained by the substitution of bigger Zr^{4+} cations (radius 0.84 Å) by smaller Ti^{4+} cations (radius 0.74 Å), which might result in higher bond strength. These peak shifts are also observed for the TaYSZ sample. The peak at 260 cm⁻¹ is shifted to 320 cm⁻¹ while the peak at 640 cm⁻¹ is shifted to 665 cm⁻¹. This uneven shifting can be explained by a different cation surrounding in TaYSZ compared to 7YSZ or TiYSZ. In TaYSZ, the smaller Ta^{5+} ion adopts the tetrahedral coordination compared to octahedrally coordinated Zr^{4+} or Y^{3+} cations. This brings higher disparity between the Zr-O′ bonds and the Zr-O bonds and hence the peak shift due to Zr-O′ (260 cm⁻¹) is much higher compared to the shift of the peak due to Zr-O bond (640 cm⁻¹).
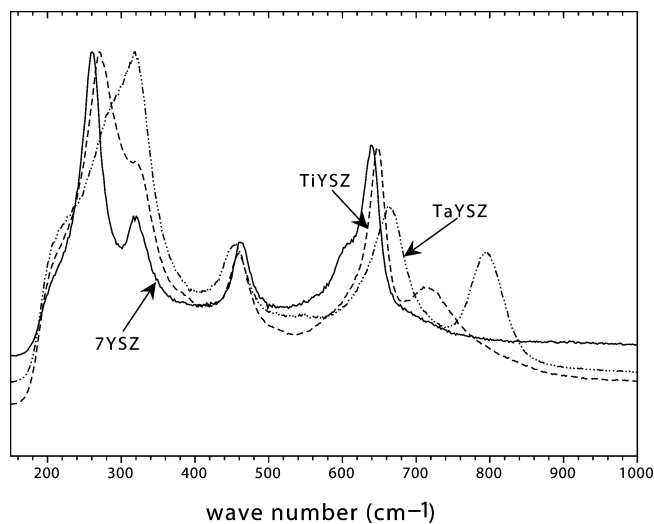

Fig. 1 : Raman spectra of TaYSZ, 7YSZ and TiYSZ samples.

TaYSZ annealed at temperatures below 1500 °C shows two additional peaks at 418 and at 510 cm⁻¹ (see Fig. 2). According to the XRD analysis of TaYSZ treated at different temperatures, shown in Fig. 3, this peak should correspond to m-$YTaO_4$ phase. XRD patterns of TaYSZ samples show tetragonal phase as the major component with minor $YTaO_4$ content, $YTaO_4$ disappearing at 1500 °C. This is consistent with previous observations [6,7].

In order to identify these extra Raman peaks in TaYSZ spectra, Raman spectroscopy of pure $YTaO_4$ has been performed, Fig. 2. Peaks at 420 and 518 cm⁻¹ are characteristic of monoclinic $YTaO_4$ phase. All other peaks of $YTaO_4$ are not seen in the TaYSZ spectrum, probably because they overlap with the characteristic TaYSZ peaks, giving asymmetry to the peak shapes. Overlapping of these peaks could also result in the broad peaks in the spectrum of the TaYSZ samples treated below 1500 °C. These extra $YTaO_4$ peaks are not found in the spectrum of the TaYSZ sample treated at 1500 °C, consistent with the XRD observation where $YTaO_4$ phase disappears at 1500 °C. Fig. 2 also shows shifting of the peaks at 260 and 640 cm⁻¹ to higher wave numbers with increasing temperature. This again indicates higher $YTaO_4$ dissolution

in the ZrO_2 lattice as the temperature rises. With increase in temperature, more of $YTaO_4$ goes into the solid solution leading to higher disparity between Zr-O′ and Zr-O bonds. Again, sharpening of the peaks with increase in temperature shows higher ordering in the lattice. This highly ordered tetragonal structure is the reason for the high-temperature stability of TaYSZ.
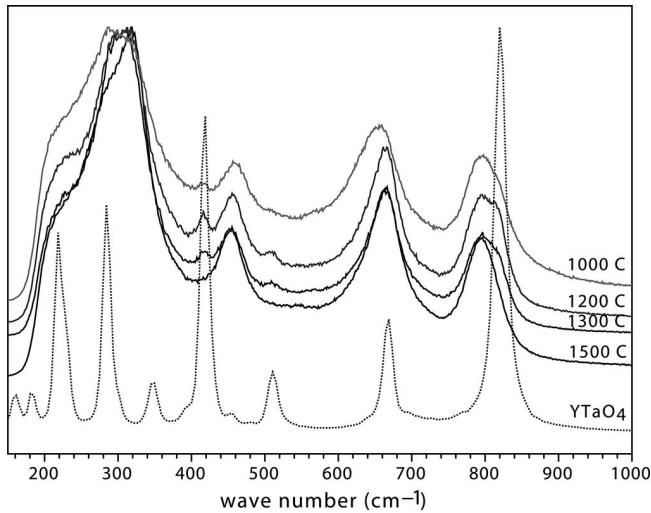

Fig. 2 : Raman spectra of the TaYSZ sample at different temperatures. The spectrum of $YTaO_4$ is also included.
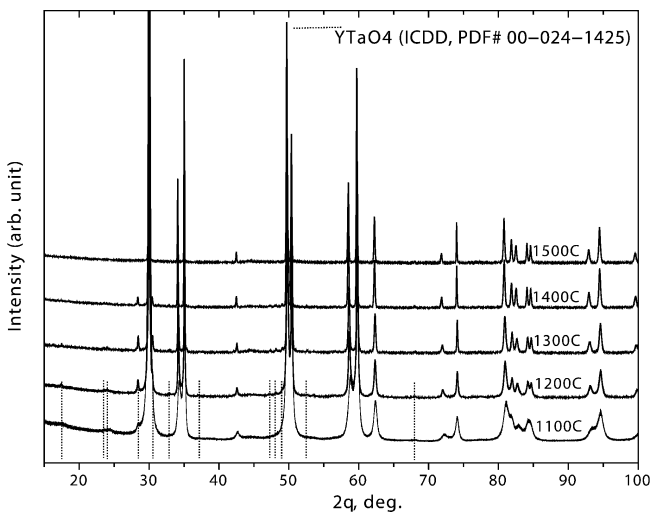

Fig. 3 : XRD patterns of the TaYSZ sample treated at different temperatures.

CaYSZ synthesized by means of reverse coprecipitation and solid state synthesis as well as commercially obtained CaSZ samples show a single-phase cubic structure (see Fig. 4). However, Raman spectroscopy on the CaSZ commercial sample also shows tetragonal Raman peaks and m-ZrO_2 peaks at some spots along with cubic peaks. CaSZ with 5 mol% CaO is known to have a cubic structure with minor m-ZrO_2 [13]. It can be assumed that this tetragonal phase is identical to t″ phase and hence remains undetected by XRD. Raman spectra of all the CaYSZ samples and the CaSZ sample are shown in Fig. 5. Raman spectra of monoclinic ZrO_2 phases present in the CaSZ sample have not been shown here. Element composition along with Raman peak position and XRD peak position of 2θ=30° of each of the systems are given in Table 1. In a comparison of the Raman peak shift of the cubic component of each system, it can be seen that with higher Ca^{2+} ion doping, the peak shifts to a lower wave number. This is due to the larger ionic radii of Ca^{2+} ions compared to Zr^{4+} ions, which increases the bond length and hence decreases the bond energy. A similar effect was observed on comparing the effect of Y^{3+} addition. The effect of Y^{3+} ion doping on the Raman shift is much less pronounced compared to the effect of Ca^{2+} doping. The XRD pattern also shows a peak shift to lower 2θ when the dopant concentration is increased, as can be seen from the insert in Fig. 4. Peak shifting to lower 2θ is due to an increase in the lattice parameter (see Table 1) with addition of Y^{3+} and/or Ca^{2+} ions.
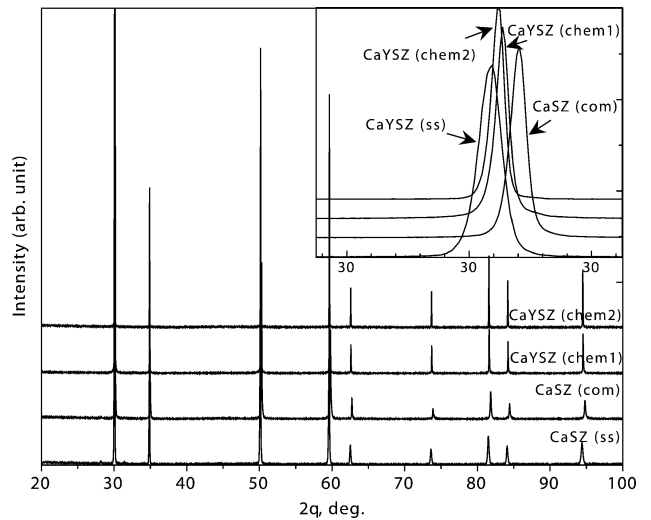

Fig. 4 : XRD pattern of Ca(Y)SZ samples. The insert shows the peak shifts at 2θ = 30°.

Table 1: Composition, Raman peak positions and 2θ position of XRD peak (30°) of the studied Ca(Y)SZ samples.

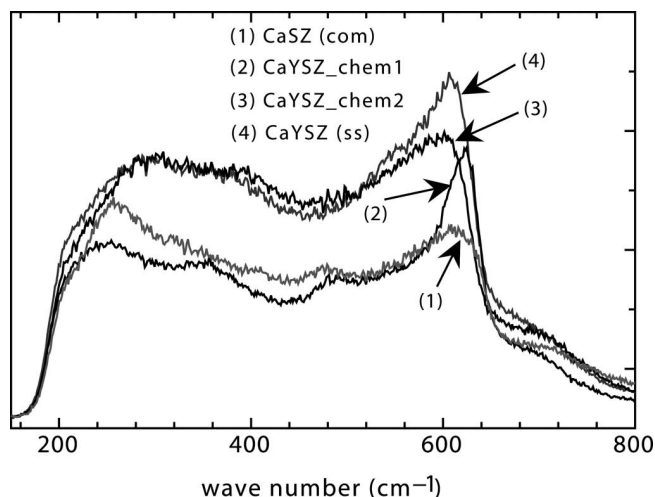| Sample	Ca(at%)	Y(at%)	Zr(at%)	Raman peak position	Lattice parameter (Å)	XRD 2θ ≈ 30° peak position
CaSZ (commercial)	5	0	95	610	5.129	30.17
CaYSZ (chem1)	1.77	17.69	80.54	626	5.137	30.11
CaYSZ (chem2)	9.42	11.04	79.54	606	5.139	30.10
CaYSZ (solid state)	4.75	16.6	78.65	608	5.143	30.08

Fig. 5 : Raman spectra of Ca(Y)SZ systems.

IV. Conclusions

Phase evolution of ZrO_2 on doping with Ta-Y, Ti-Y and Ca-Y ions has been characterized with Raman spectroscopy and X-ray powder diffraction. Ta^{5+}/Ti^{4+} doping shifts the 260 and 640 cm^{-1} Raman peaks of YSZ to higher wave numbers, indicating decreased Zr-O′ and Zr-O bond lengths. Uneven shifting of these peaks in the case of the TaYSZ sample was observed, which can be explained by the local change in the metal atoms surrounding. TaYSZ annealed at a lower temperature than 1500 °C always contained minor $YTaO_4$ phase, which was confirmed by means of Raman spectroscopy. CaYSZ was cubic in symmetry and increased doping of Ca or Y shifts the peaks to a lower wave number. The peak shift was more pronounced on doping with Ca^{2+} ion compared to that on doping with Y^{3+} ion.

References

1   Levi, C.G.: Emerging materials and processes for thermal barrier coatings, *Curr. Opin. Solid St. M.*, **8**, 77 – 91, (2004).

2   Jones, R.L., Mess, D.: Improved tetragonal phase stability at 1400°C with Scandia, yttria-stabilized zirconia, *Surf. Coat. Tech.*, **86 – 87**, 94 – 101 (1996).

3   Miller, R.A., Smialek, J.L., Garlick, R.G.: Science and technology of zirconia, Am. Ceram. Soc., Inc., Columbus, OH, **241**, (1981).

4   Cainery, J.M., Rebollo, N.R., Ruehle, M., Levi, C.G.: Phase stability of thermal barrier Oxides: a comparative study of Y and yb additions, *Int. J. Mat. Res.*, **98**, 12, 1177 – 1187, (2007).

5   Schaedler, T.A., Leckie, R.M., Kraemer, S., Evans, A.G., Levi, C.G.: Toughening of non-transformable t′-YSZ by addition of titania, *J. Am. Ceram. Soc.*, **90**, 3896 – 3901, (2007).

6   Kim, D.J., Tien, T.Y.: Phase stability and physical properties of cubic and tetragonal ZrO_2 in the system ZrO_2-Y_2O_3-Ta_2O_5, *J. Am. Ceram. Soc.*, **74**, 3061 – 3065, (1991).

7   Pitek, F.M., Levi, C.G.: Opportunities for TBCs in the ZrO_2-$YO_{1.5}$-$TaO_{2.5}$ system, *Surf. Coat. Technol.*, **201**, 6044 – 6050, (2007).

8   Keramidas, V.G., White, W.B.: Raman scattering study of the crystallization and phase transformations of ZrO_2, *J. Am. Ceram. Soc.*, **57**, [1], 22 – 24, (1974).

9   Yashima, M., Ohtake, K., Kakihana, M., Arashi, H., Yoshimura, M.: Determination of tetragonal-cubic phase boundary of $Zr_{1-x}R_xO_{2-x/2}$ (R= nd, sm, Y, er and Yb) by raman scattering, *J. Phys. Chem. Solids*, **57**, [1], 17 – 24, (1996).

10 Kim, D.J., Jung, H.J., Yang, I.S.: Raman spectroscopy of tetragonal zirconia solid solutions, *J. Am. Ceram. Soc.*, **76**, [8], 2106 – 2108, (1993).

11 Michel, D., Van Den Borre, M.T., Ennaciri, A.: Vibrational spectra and force fields of tetragonal zirconia and zirconium germinates, p. 555 – 62 in Advances in Ceramics, Vol. 24, Science and Technology of Zirconia III, edited by S. Somiya, N. Yamamoto and H. Yanagida. American Ceramic Society, Westerville, OH, (1988).

12 Thackery, D.P.S.: The raman spectrum of zirconium dioxide, *Spectrochim. Acta A*, **30**, 549 – 550, (1974).

13 Garvie, R.C., Nicholson, P.S.: Phase analysis in zirconia systems, *J. Am. Ceram. Soc.*, **55**, [6], 303 – 305, (1972).